# Chapter 4
# Biomechanical Considerations in Arthritis of the Hip

**Agnes G. d'Entremont, Lawrence L. Buchan, and David R. Wilson**

## Introduction

Biomechanics plays a role in the etiology of hip arthritis and in its treatment. The objective of this chapter is to summarize our current understanding of hip biomechanics as it relates to arthritis.

## Biomechanical Quantities and Their Importance

Biomechanics includes many quantities that are important in describing elements of hip function.

**Kinematics** describes movement of the joint. Range of motion is often used to summarize kinematics, and is important as an indicator of hip function, since the

A.G. d'Entremont, PhD
Department of Mechanical Engineering, University of British Columbia, 2054-6250 Applied Science Lane, Vancouver, BC, Canada V6T 1Z4
e-mail: agnes.dentremont@mech.ubc.ca

L.L. Buchan, BASc, MASc
Biomedical Engineering Program, Centre for Hip Health and Mobility, Vancouver Coastal Health Research Institute, University of British Columbia, 678G-2635 Laurel St, Robert H. N. Ho Research Centre, Vancouver, BC, Canada V5Z 1M9
e-mail: lawrence.buchan@alumni.ubc.ca

D.R. Wilson, BEng, DPhil (✉)
Department of Orthopedics, Centre for Hip Health and Mobility, Vancouver Coastal Health Research Institute, University of British Columbia, Rm 3114, 910 W. 10th Avenue, Vancouver, BC, Canada V5Z 1M9
e-mail: david.wilson@ubc.ca



R.K. Aaron (ed.), *Diagnosis and Management of Hip Disease*,
DOI 10.1007/978-3-319-19905-4_4

hip's substantial range of motion in all three anatomical planes is required for normal body movement. Reductions in range of motion are important because they may limit activity, and also because they may be signs of mechanical disruption at the joint itself which has further consequences on joint function, such as impingement of the femur on the acetabulum.

**Resultant force** on the hip and its line of action affects function as well. For example, there is a strong relationship between hip forces and muscle forces.

**Stress** describes how forces are distributed within a material, such as cartilage or bone. Contact stress describes how forces are distributed in a region of contact, such as between femoral and acetabular cartilage. Abnormal contact stress is widely believed to predispose a joint to osteoarthritis [1].

**Joint fluid pressure** is measured within the joint's synovial fluid, which is sealed in by the acetabular labrum. Loading the hip increases the pressure in this fluid, which plays a role in distributing load across the cartilage surface. Loss of pressure may reflect damage to the labral seal and disrupted patterns of contact stress.

## Methods of Biomechanical Assessment

Biomechanics can be assessed using ex vivo experiments, in vivo measurements, and mathematical models. Each approach has strengths and limitations.

Biomechanics is studied ex vivo by instrumenting cadaver hips and then subjecting them to simulations of physiological movement and loading. The key advantage to this approach is that many mechanical quantities of interest—such as kinematics, resultant force, and contact stress—can be measured. A leading limitation of this approach is that substantial simplifications of the dynamic nature of activity are usually required (such as limited numbers of muscles, static postures, and limited ranges of motion).

Biomechanics is studied in vivo by making measurements in living participants. Motion analysis systems measure movement of the limb segments and external forces. Instrumented prostheses measure resultant force at the hip during activity. The key advantage of in vivo approaches is that measurements are made during real physiological activity. Two leading limitations of this approach are that many important mechanical quantities, such as contact stress on the cartilage surface, cannot be measured in vivo, and deformities and disorders cannot be simulated.

Mathematical models predict hip biomechanics from inputs such as joint geometry and mechanical properties of tissues. A key advantage of this approach is that a broad range of disorders and treatments can be simulated. The leading limitation of models is that many simplifications of joint properties must be made, and the impact of these simplifications on model predictions is often not known. Model predictions may therefore be poor reflections of hip biomechanics in vivo.

## Biomechanics of Stabilizing Structures

The acetabular labrum is frequently torn. The biomechanics of the labrum and other stabilizing structures have been studied because of potential links between labral tears and osteoarthritis.

### *Range of Motion and Stability*

Simulated circumferential and radial tears of the labrum did not affect the stability ratio (peak dislocation force/compressive force) in 22 cadaver hip specimens [2], but substantial labrectomy significantly decreased the stability ratio. Large circumferential tears of the labrum increased strain (reflecting increased stress) in the anterior labrum for combined anterior and compressive loads, while radial tears decreased strain in the anterior and anterior-superior labrum.

Sectioning the iliofemoral ligament increased external rotation and anterior translation in response to a standardized torque in 15 cadaver specimens [3], which led the authors to conclude that this structure plays a significant role in limiting external rotation and anterior translation of the femur.

Sectioning the labrum alone did not increase external rotation in response to a standardized torque [3] in 15 cadaver hips, but both external rotation and anterior translation were larger when both the labrum and the iliofemoral ligament were sectioned than when the iliofemoral ligament alone was sectioned, leading the authors to conclude that the labrum provides a secondary stabilizing role for external rotation and anterior translation. The impingement test (combined flexion, adduction and internal rotation) increased strain (reflecting increased stress) in the anterolateral labrum in 12 cadaver specimens [4], and other tested postures produced strain changes in other parts of the labrum. In a study of seven cadavers, five different loading maneuvers all produced strain in the anterosuperior part of the labrum. Maximum strains averaged 13.6 % in the axial direction and 8.4 % in the circumferential direction [5].

### *Pressure and Stress*

In three loaded cadaver hips, resecting the labrum reduced the fluid pressure in the joint and speeded up cartilage compression, suggesting that the labral seal plays a key role in normal force distribution in the joint [6]. In an MRI study of six cadaver hips, labral repair caused a 2 % decrease in mean cartilage strain (reflecting contact stress) compared to a torn labrum, and labral resection caused a 6 % increase in maximum cartilage strain compared to labral repair [7]. These

findings suggest that the labral seal should be preserved whenever possible, and that its disruption may predispose the joint to osteoarthritis by increasing contact stress on the joint.

## Biomechanical Effect of Problems in Acetabular Coverage

### *Developmental Dysplasia of the Hip*

Developmental dysplasia of the hip (DDH) is a condition where the infant hip is dislocated and can be reduced, or can be provoked to dislocate, and has primarily acetabular anatomic abnormalities [8]. DDH is characterized by poor coverage of the acetabulum over the femoral head [9]. This condition is associated with early hip osteoarthritis.

#### Range of Motion

In an experimental study of hip range of motion, hips with unreduced developmental dysplasia (four hips) had slightly higher internal/external rotation ROM (combined with flexion/extension), and slightly lower abduction ROM, compared to a group of 325 normal children (Fig. 4.1) [10].

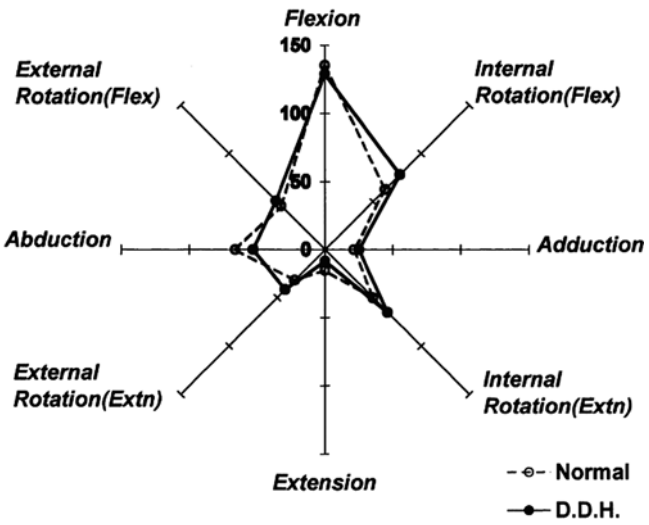


**Fig. 4.1** Measured range of motion in normal children and children with DDH. [Reprinted from Rao KN, Joseph B. Value of Measurement of Hip Movements in Childhood Hip Disorders. J Pediatr Orthop [Internet]. 2001;21(4):495–501. With permission from Wolters Kluwer Health.]

### Stress

Generally, the results from mathematical models show that higher hip contact stress is associated with more severe deformity and less positive outcomes. Increased deformity was associated with increased peak contact stress (Severin 1a and 1b: 2.3 MPa; Severin 2a and 2b: 2.4 MPa; Severin 3: 4.6 MPa) in a study using models whose geometry came from AP radiographs for 35 patients [11]. Peak stresses in both the femur and acetabulum increased with increasing deformity [12] in a study using a three-dimensional finite element analysis (FEA) of a CT-based normal hip joint model which was deformed to simulate three severities of DDH. Peak contact stress increased in hips with less acetabular coverage when the abductor muscle force became more vertical in models of dysplastic hips based on modifications to normal 2D models created from AP radiographs [13].

A study that used planar models from X-rays combined with duration of follow-up (mean 29 years) to calculate accumulated stress over time in 89 DDH hips identified a damage threshold of 10 MPa-years, finding that 80.9 % of all hips below the threshold had good outcomes based on Severin classifications, and 90.4 % of all hips above the threshold had poor outcomes [14]. Two non-uniform contact stress models based on longitudinal radiographic information from the same 89 DDH hips showed an association between higher loads and worse clinical outcomes, although the damage thresholds (based on clinical outcomes) were very different for the two models (2.0 MPa versus 4.5 MPa) [15].

Mathematical models have shown that various osteotomies used to treat DDH reduce peak stress or contact stress. Models based on radiographs showed that the Tonnis osteotomy for insufficient coverage and avascular necrosis of the femoral head reduced peak normalized contact stress by 55.9 % (peak stress/BW) in 75 patients [16]. A 2D model showed that triple osteotomy of the innominate bone decreased contact stress and increased contact area, although not to the level of normal controls [17]. A 3D model showed that the Bernese periacetabular osteotomy for residual dysplasia increased the normalized resultant hip force but reduced the peak contact stress normalized by BW from 5.2 to 3.0 kPa/N due to increased coverage [18]. Better long-term clinical outcomes were observed in hips with lower postoperative normalized peak stress [18]. The same 3D FEA model mentioned above was used to simulate a Bernese periacetabular osteotomy in each severity level of DDH. Peak stresses were found to decrease with osteotomy in both the femur and acetabulum, although none were reduced to the level of the normal model, and more severe deformity was associated with higher stress following osteotomy [12].

### Force

Salter osteotomy reduced the measured resultant joint force on the hip from 2.7 BW (583 N) to 1.2 BW (266 N) in a plastic model of a patient's DDH joint created with rapid prototyping [19]. Mean gluteus maximus force was similarly reduced from 0.46 BW (100 N) to 0.24 BW (52 N).

## *General/Focal Acetabular Overcoverage*

General acetabular overcoverage is characterized by a very deep acetabulum or circumferentially prominent acetabular rim [20]. Coxa profunda and protrusio acetabuli are defined by overlapping of the ilioischial line medial to the acetabular fossa or femoral head, respectively, on an AP radiograph. A center-edge (CE) angle below 25° is associated with dysplasia, while a CE angle above 39° describes overcoverage [20, 21].

The main biomechanical failure mechanism in general overcoverage (coxa profunda/protrusio acetabuli) is hypothesized to be dynamic pincer-type femoroacetabular impingement, which is associated with osteoarthritis. General acetabular overcoverage is often referred to as a pincer deformity. The mechanism of pincer impingement is thought to be characterized by linear contact of the femoral head-neck junction against the acetabular rim and labrum [22, 23]. Chondrolabral damage patterns related to pincer morphology are widely distributed around the acetabulum [24].

Focal acetabular overcoverage is characterized by a prominence of the acetabular rim in a specific location, and is often related to acetabular retroversion. In retroversion, the acetabular opening is oriented more posteriorly than normal [25]. Clinically, retroverted acetabula are commonly associated with posterior cartilage damage and anterior impingement-related chondrolabral pathology [25–27]. Retroversion is often indicated by the cross-over sign on a plain A-P radiograph, or can be determined using 3D CT [28].

As with general overcoverage, the main biomechanical mechanism of concern in retroverted hips is thought to be pincer impingement at the anterior rim. Therefore, retroversion is frequently combined with protrusio/profunda in the pincer impingement literature. It is important to note that some retroverted acetabula are associated with deficient posterior coverage [28, 29], and subsequently may have different static loading patterns compared to profunda/protrusio acetabula.

### Range of Motion

In an in vivo study, 32 hips with cam or pincer pathoanatomy had a mean internal rotation ROM at 90° flexion of 4° ± 8° (range: −10° to 20°) compared to 28° ± 7° (range: 10–40°) in 40 control hips [30]. This study also quantified the neck-rim relationship on open-configuration MRI scans taken with hips in 90° of flexion using the $\beta$ angle, defined by a line connecting the femoral head center to the head-neck junction, and a line connecting the femoral head center to the acetabular margin (Fig. 4.2). The mean $\beta$ angle was only 5° ± 9° in the cam or pincer subjects compared to 30° ± 9° in the controls. This work supports the hypothesis that linear abutment of the head-neck junction against the acetabular rim (impingement) terminates motion.

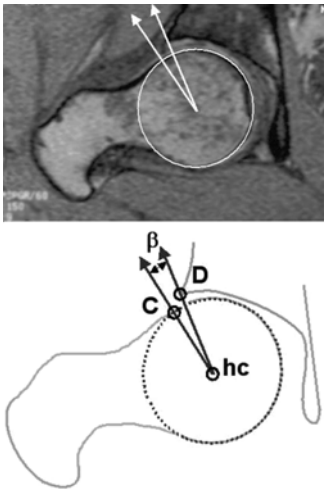


**Fig. 4.2** (*Top*) Definition of the $\beta$ angle on an MR image (*Bottom*) and on a diagram. [Reprinted from Wyss TF, Clark JM, Weishaupt D, Nötzli HP. Correlation between internal rotation and bony anatomy in the hip. Clin Orthop Relat Res [Internet]. 2007 Jul [cited 2013 Feb 5];460(460):152–8. With permission from Wolters Kluwer Health.]

Computer models confirm that most types of cam and/or pincer pathomorphology lead to reductions in flexion, internal rotation, abduction, and internal rotation at high flexion, although pincer and cam deformity have often been assessed together. Internal rotation at 90° flexion, a representation of the anterior impingement test, is commonly simulated with these models because it is thought to bring the anterior femoral head-neck junction close to the anterosuperior quadrant of the acetabular rim (often the most prominent part of the rim and a common site for chondrolabral pathology).

In a study using a mathematical model, 31 symptomatic hips with cam or pincer pathoanatomy (12 cam, 7 pincer, 12 mixed) had significantly decreased flexion, internal rotation at 90° of flexion, and abduction compared to a control group of 36 hips [31]. The same model was used to predict the location of impingement during internal rotation at high flexion in six hips with pincer deformities. The predicted impingement site for the pincer group was highly localized anterosuperiorly, whereas the actual site of chondral and labral damage observed in a separate group of 16 pincer hips spanned nearly the entire superior portion of the acetabulum and extended inferiorly [24].

Another model predicted that a group of 10 pure cam hips, 8 pure pincer hips, and 10 with combined cam/pincer pathoanatomy had limited flexion, internal rotation, abduction and internal rotation at 90° of flexion compared to 33 normal hips. The model predicted impingement on the anterosuperior quadrant of the acetabular rim for both control and FAI hips, with minimal difference in impingement zones between cam/pincer/combined hips [32].

Models of 50 hips undergoing arthroscopy for FAI showed that increased acetabular retroversion (simulated with increased anterior tilt) decreased internal rotation

ROM by 5.9° at 90° flexion, and by 8.5° at 90° flexion plus 15° adduction. Increased retroversion shifted the predicted impingement zone anteriorly. Increased acetabular anteversion (simulated with increased posterior tilt) increased internal rotation ROM by 5.1° at 90° flexion, and by 7.4° in FADIR [33].

### Stress

Using idealized hip geometry in a finite element model, Chegini et al. evaluated the effects of varying $\alpha$ angles (40–80° range at 10° intervals) and center-edge (CE) angles (0–40° range at 10° intervals) on hip joint contact stress and acetabular cartilage stress during stand-to-sit and walking from heel-strike to toe-off [34]. Overcoverage reduced contact stress and chondral stress, while dysplasia greatly increased contact stress and chondral stress. Peak joint contact stress as well as chondral stress was inversely related to CE angle. Conversely, at deep flexion during stand-to-sit, a high $\alpha$ angle in combination with a high CE angle yielded the highest contact stress and acetabular chondral stress (Fig. 4.3). Cartilage stress distribution in the mixed cam-pincer hip during stand-to-sit was concentrated in the anterosuperior quadrant, where intraoperative cartilage damage is often observed (Fig. 4.4).

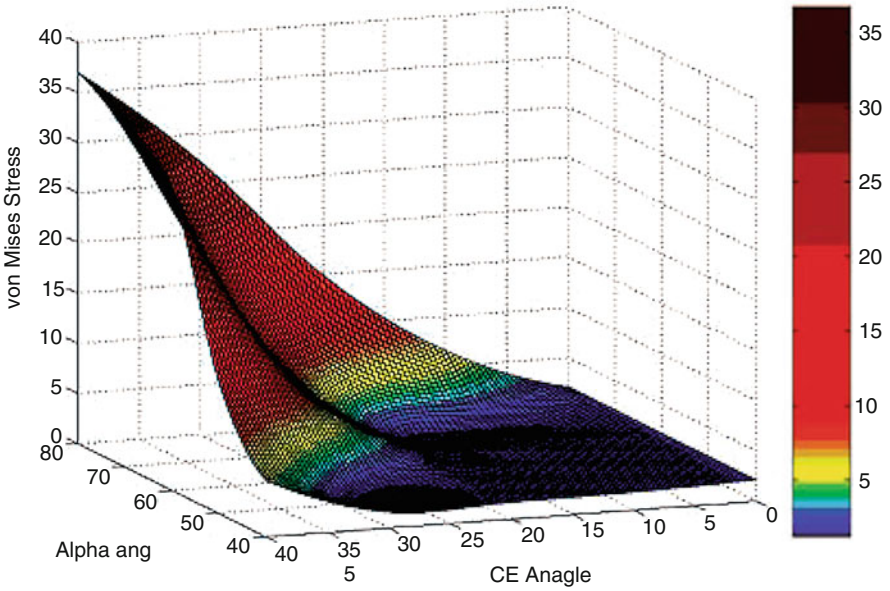


**Fig. 4.3** Effect of CE angle and alpha angle on maximum von Mises stress in acetabular cartilage during stand-to-sit. [Reprinted from Chegini S, Beck M, Ferguson SJ. The effects of impingement and dysplasia on stress distributions in the hip joint during sitting and walking: a finite element analysis. J Orthop Res [Internet]. 2009 Feb [cited 2014 Jun 18];27(2):195–201. With permission from John Wiley & Sons, Inc.]

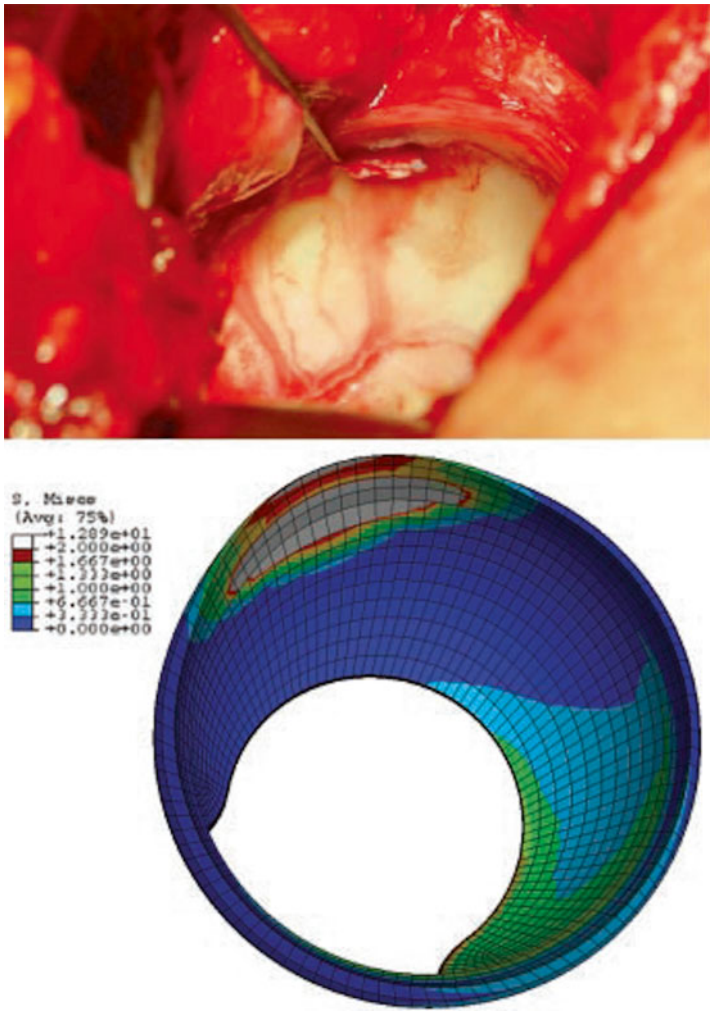


**Fig. 4.4** (*Top*) Intraoperative image of cartilage damage in a cam-type hip. (*Bottom*) Cartilage stress distribution predicted by a model of a typical cam-type hip during stand-to-sit. [Reprinted from Chegini S, Beck M, Ferguson SJ. The effects of impingement and dysplasia on stress distributions in the hip joint during sitting and walking: a finite element analysis. J Orthop Res [Internet]. 2009 Feb [cited 2014 Jun 18];27(2):195–201. With permission from John Wiley & Sons, Inc.]

These results indicate that generally overcovered hips are likely not at risk for highly stressed posterior acetabular cartilage.

The applied forces and resulting peak stresses (3.3–16.5 MPa) from this model are within the same range reported by studies using CT-based patient-specific geometry for normal hips [35–38]. The contact stress magnitudes are consistent with experiments where miniature pressure transducers implanted

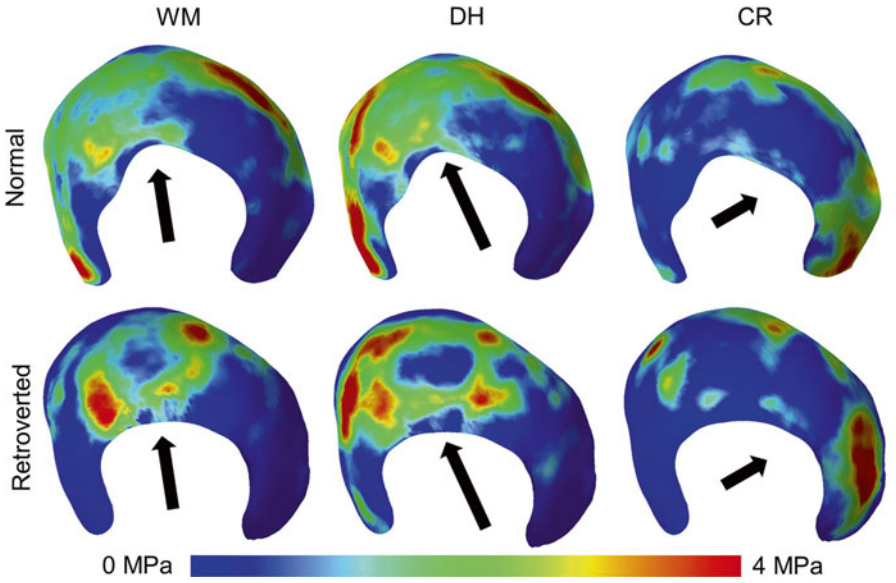


**Fig. 4.5** Acetabular contact stress predictions for normal and retroverted hips for walking mid-stride (WM), descending stairs (DH) and chair rising (CR). The arrows indicate the approximate direction and relative magnitude of the load during each activity. [Reprinted from Henak CR, Carruth ED, Anderson a E, Harris MD, Ellis BJ, Peters CL, et al. Finite element predictions of cartilage contact mechanics in hips with retroverted acetabula. Osteoarthritis Cartilage [Internet]. Elsevier Ltd; 2013 Oct [cited 2014 Jun 17];21(10):1522–9. With permission from Elsevier.]

superficially into normal cadaver femoral head cartilage measured average peak contact stress in femoral cartilage to be 8.8 MPa for an applied vertical force load of 2700 N [39].

Subject-specific finite element models showed that contact stress was concentrated in the superomedial (SM) region in retroverted acetabula, while normal hips had more widely distributed contact stresses (Fig. 4.5). During walking and stair descent, normal hips had 2.6–7.6 times larger contact stresses in the posterolateral (PL) acetabulum. Conversely, retroverted hips had 1.2–1.6 times larger contact stresses in the superomedial acetabulum [37]. The authors suggest that these results refute the theory of high posterior stresses in retroverted acetabula due to decreased posterior coverage. A lack of concentrated loads on the posterior acetabulum suggests that retroverted hips with cartilage degradation on the posterior acetabulum may more likely be due to levering and "contre-coup" contact, rather than static posterior overload.

## *Posterior Overcoverage: Acetabular Anteversion*

Acetabular anteversion is characterized by an acetabular opening that projects anteriorly. A prominent posterior wall may be associated with acetabular anteversion and might reduce the available bony range of extension and external rotation. Further,

the anterior wall might be deficient and lead to overload. However, we found no biomechanics studies that evaluated the effects of posterior overcoverage.

## Biomechanical Effect of Problems in Femoral Neck Orientation

### *Femoral Anteversion and Coxa Valga*

A valgus femur, or femur with coxa valga, is characterized by a caput-collum-diaphyseal (CCD) angle greater than 135° [40, 41]. Coxa valga is hypothesized to arise secondary to DDH and as such is associated with concentrated stresses on the acetabular roof. Femoral anteversion (or antetorsion) is characterized by a posteriorly oriented femoral neck, which is closer than normal to the posterior acetabulum and related acetabular structures. Recent work has focused on dynamic posterior impingement-related considerations in coxa valga and femoral anteversion.

#### Range of Motion

In an experimental study in children, hips with femoral anteversion had reduced external rotation in extension and abduction compared to normal subjects (Fig. 4.6) [10].

Mathematical models predicted reduced adduction, extension and external rotation range of motion in hips with both coxa valga and anteversion [42]. External rotation at 90° of flexion was also limited. These findings are consistent with experimental measurements of hip range of motion [10, 40]. The authors suggested that femurs with both coxa valga and anteversion are predisposed to a reduced range of external rotation and extension due to posterior extra-articular impingement. The findings suggest that hips with coxa valga and high femoral anteversion are at substantial risk for posterior impingement, and that treatment decisions involving coxa valga/anteversion should consider dynamic pathology in addition to static overload. Extra-articular structures like the anterior inferior iliac spine, ischial tuberosity, greater trochanter, and lesser trochanter caused terminal impingement much more frequently in the coxa valga/anteversion group than in the control group. The authors postulate that posterior impingement may induce a levering effect and eventually cause “contre-coup” chondrolabral lesions on the anterosuperior acetabulum—which would explain positive anterior impingement tests.

### *Femoral Retroversion and Coxa Vara*

Coxa vara is characterized by a caput-collum-diaphyseal (neck-shaft) angle less than 125° [43, 44]. In coxa vara, the superior margin of the femoral neck is closer than normal to the anterosuperior acetabulum and therefore associated with loss of

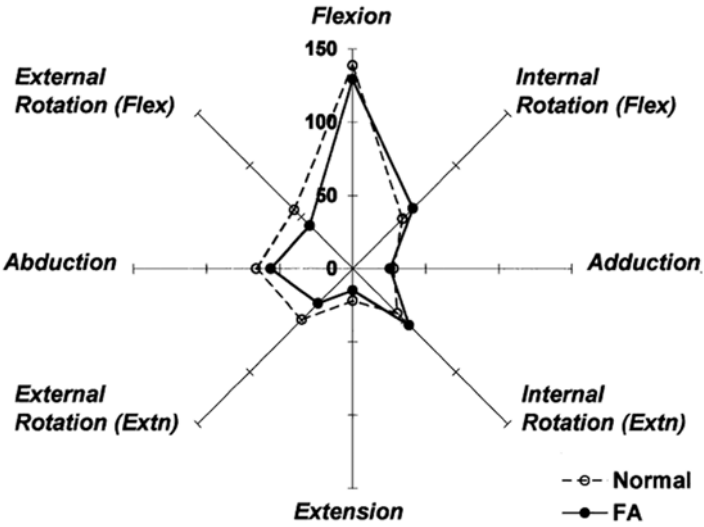


**Fig. 4.6** Measured range of motion in hips with femoral anteversion (FA) and normal hips. [Reprinted from Rao KN, Joseph B. Value of Measurement of Hip Movements in Childhood Hip Disorders. J Pediatr Orthop [Internet]. 2001;21(4):495–501. With permission from Wolters Kluwer Health.]

hip ROM. Similarly, femoral retroversion (or retrotorsion) brings the anterior margin of the femoral neck closer to the anterosuperior acetabulum. Femoral version is defined in the axial or transverse plane by the angle between the femoral neck axis proximally and intercondylar line distally.

## Range of Motion

Experimental measurements showed reduced abduction, internal rotation, and external rotation ROM in hips with infantile coxa vara compared to normals (Fig. 4.7) [10]. Hips with femoral retroversion had reduced internal rotation ROM and increased external rotation ROM compared to normals (Fig. 4.8) [10]. Hips with combined retroversion and coxa vara had substantially reduced abduction and internal rotation ROM and slightly increased external rotation than normal (Fig. 4.9) [10].

Although it is not clear that bony collisions terminate motion, this work demonstrates that abnormal morphology that brings the femoral neck closer to the acetabular rim in a specific plane is associated with limited ROM in that plane. In coxa vara, the femoral neck is brought closer to the superior acetabulum in the coronal plane, and likewise motion towards the superior acetabulum in the coronal plane—abduction—is limited. Similarly in retroversion, the femoral neck is brought closer to the anterior acetabulum, and likewise motion towards the anterior acetabulum in the axial plane—internal rotation—is limited. For this reason, it is hypothe-

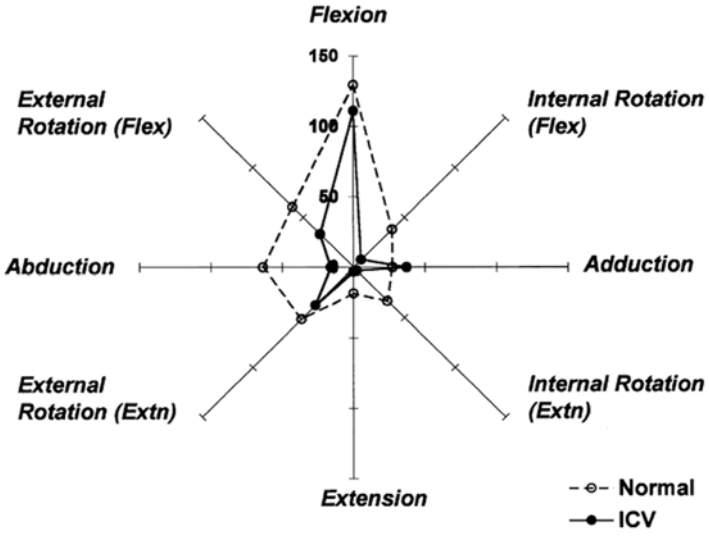


**Fig. 4.7** Range of motion in normal hips and hips with infantile coxa vara (ICV). [Reprinted from Rao KN, Joseph B. Value of Measurement of Hip Movements in Childhood Hip Disorders. J Pediatr Orthop [Internet]. 2001;21(4):495–501. With permission from Wolters Kluwer Health.]

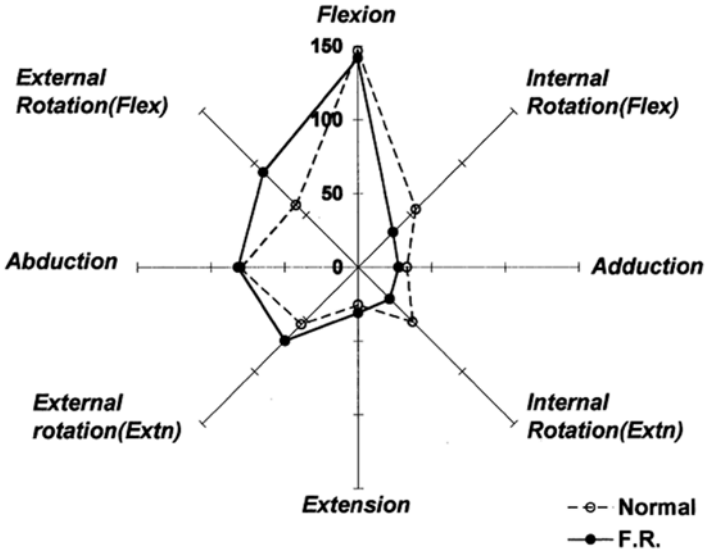


**Fig. 4.8** Range of motion in normal hips and hips with femoral retroversion (FR). [Reprinted from Rao KN, Joseph B. Value of Measurement of Hip Movements in Childhood Hip Disorders. J Pediatr Orthop [Internet]. 2001;21(4):495–501. With permission from Wolters Kluwer Health.]

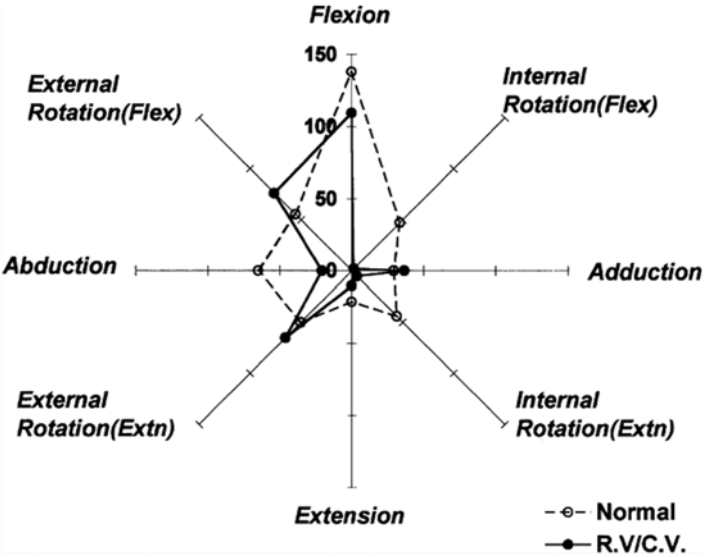


**Fig. 4.9** Range of motion in normal hips and hips with coxa vara and femoral retroversion (R.V./C.V.). [Reprinted from Rao KN, Joseph B. Value of Measurement of Hip Movements in Childhood Hip Disorders. J Pediatr Orthop [Internet]. 2001;21(4):495–501. With permission from Wolters Kluwer Health.]

sized that coxa vara and femoral retroversion increase the likelihood of linear impact of the femoral neck against the acetabulum (i.e., pincer impingement) occurring during daily activity.

## Biomechanical Effect of Problems at the Femoral Head-Neck Junction

### *SCFE*

Slipped capital femoral epiphysis (SCFE) is a primarily adolescent disorder where the epiphysis slips in an inferior and posterior direction along the growth plate or physis, resulting in a femoral deformity believed to lead to acetabular impingement and cartilage damage [45].

#### Range of Motion

SCFE is expected to cause loss of ROM due to impingement of the deformed femoral head or neck on the acetabulum.

In a study using computer models from 31 SCFE patients and 15 contralateral controls [46], mild slips (as defined by Southwick angle) generally showed similar or slightly reduced ROM compared to controls (e.g., flexion: mild SCFE 89°, normal 99°), while severe slips had drastic reductions in ROM (e.g., flexion: severe SCFE 4°). For mild SCFE with a more prominent head-neck junction (type 2), ROM was further decreased (e.g., flexion: mild SCFE (type 2) 62°). Moderate SCFE cases were associated with larger decreases in ROM (e.g., flexion: moderate SCFE 14.2°), which were worsened by prominent head-neck junctions (e.g., flexion: moderate SCFE (type 3) 2°), while severe slips were not further affected by head-neck junction morphology.

#### Stress

Finite element models for both hips from two unilateral SCFE patients (one moderate, one severe) predicted that for a moderate slip, the peak contact stress was 17 % higher and maximum stress was 29 % higher than in the contralateral hip [45]. In the severe slip, peak contact stress was 49 % higher and maximum stress was 170 % higher. Simulated subcapital osteotomy through the proximal femoral epiphysis, base-of-neck osteotomy at the neck outside the capsule, and intertrochanteric osteotomy between the greater and lesser trochanter did not change contact stress or stress for the moderate slip, while the severe case saw reductions in maximum stress by about half (along with smaller reductions in contact stress), although this was still higher than the contralateral normal hips.

### *Cam Deformity*

A cam deformity is typified by decreased concavity of the femoral head-neck junction. Cam deformities are widely thought to increase the risk of hip osteoarthritis. In 1965, Murray identified a “tilt deformity” of the femoral head and noted that radiographic tilt deformities were present in 79 out of 200 cases of hip OA [47]. In 1975, Stulberg et al. described the similar “pistol-grip deformity,” and in 1976 Solomon postulated that hip OA was secondary to such deformities [48]. In 2003, Ganz proposed that hips with tilt/pistol-grip deformities, resembling mechanical “cams,” mainly fail due to cam-type femoroacetabular impingement (Fig. 4.10) [22]. It was postulated that the cam deformity jams inside the acetabulum during forceful motion, particularly internal rotation at high flexion [22], leading to concentrated shear forces on intra-articular cartilage and acetabular labrum. The theory was largely driven by intraoperative findings from more than 600 surgical dislocations of the hip [22, 23], and evidence that patients with acetabular rim syndrome frequently have reduced concavity at the femoral head-neck junction [50, 51].

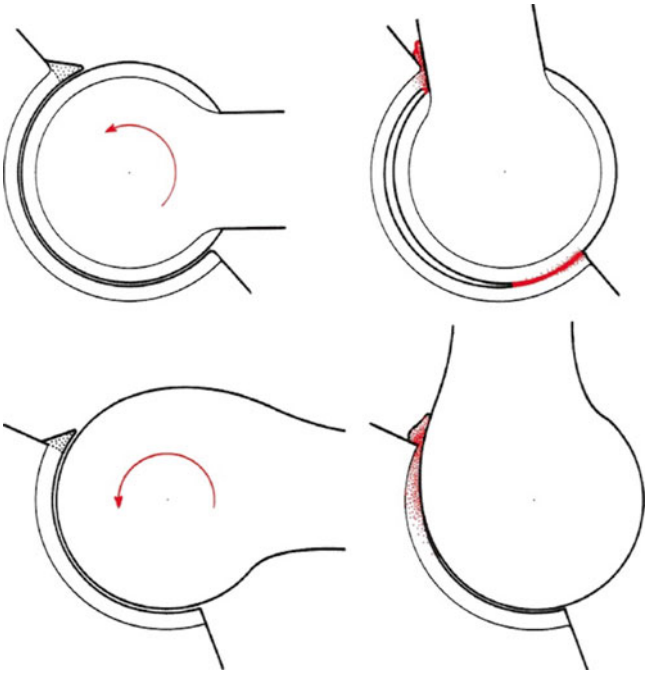

**Fig. 4.10** Schematic diagrams of cam (*top*) and pincer (*bottom*) impingement. [Reprinted from Ganz R, Leunig M, Leunig-Ganz K, Harris WH. The etiology of osteoarthritis of the hip: an integrated mechanical concept. Clin Orthop Relat Res [Internet]. 2008 Feb [cited 2014 Jul 10]; 466(2):264–72. With permission from Springer Verlag.]

Biomechanics research of the cam-type pathoanatomy has focused on measuring three main factors that are related to the cam impingement pathomechanism: (1) reductions in hip ROM caused by bony impingement; (2) other kinematic changes that might be secondary to bony collision during cam impingement; and (3) the interaction between the cam deformity and acetabulum during motion (joint contact area, joint contact stresses, and cartilage/subchondral bone stresses).

## Range of Motion

Patients with cam deformities typically present with restricted flexion, internal rotation, and abduction [52–55]. In theory, a reduced range of motion would mean a higher likelihood that cam impingement would occur in, and impede, daily activity (within the physiological range of motion). It is, however, not clear whether range of motion is dictated by bony morphology, soft-tissue constraint, or pain-related (compensatory) limits.

An experimental study of range of motion in three subgroups (symptomatic cam pathoanatomy, asymptomatic cam pathoanatomy, and controls, $n=24$ per group) showed that the symptomatic cam group had significantly reduced range of motion in all directions [56]. Notably, the asymptomatic cam group had significantly greater external rotation at neutral flexion and greater internal rotation at 90° flexion than the symptomatic group. There were no differences between symptomatic and asymptomatic groups for pure flexion and pure internal rotation. Models of 36 control hips and 12 cam, 7 pincer, and 12 mixed cam/pincer hips predicted no significant differences between cam, pincer, and combined pathoanatomies for flexion or internal rotation at 0° flexion [31].

## Location of Impingement

Several approaches have been used to link predicted location of impingement with damage on the acetabulum.

In model simulations of internal rotation tests in high flexion (at intervals from 70° to 110° flexion, combined with −20° to 20° adduction), collisions consistently occurred on the anterosuperior portion of the acetabulum in ten symptomatic subjects with cam pathoanatomy, ten asymptomatic subjects with cam pathoanatomy, and ten healthy controls [57]. In control femurs, collisions were localized on the femoral neck anteriorly, while on the cam femurs, collisions were localized more superolaterally, where the cam deformity was located.

In a study combining in vivo measurement of joint movement with model predictions of impingement location, maximum flexion, maximum internal rotation at 90° flexion, and maximum abduction produced direct impingement between the cam deformity and the acetabulum. Furthermore, engagement began at positions much earlier than the terminal position. In flexion, engagement began at 80° although the motion range was 110°, and in internal rotation at 90° flexion, engagement began at 7.2° although the motion range was 19° [58].

In a similar study using in vivo motion tracking coupled with a model to predict impingement, the anterior impingement exam (flexion around 90°, adduction, and internal rotation) led to engagement of the inferomedial portion of the femoral head-neck junction with the anterosuperior portion of the acetabulum [59]. The engagement location was consistently on the anteroinferior portion of the femoral head/neck junction, as opposed to the anterosuperior portion where cam lesion size is often at its maximum. While the accuracy and repeatability of the model are well documented [60], the study was performed in only six control hips, one cam deformity hip, one hip with general acetabular overcoverage and one hip with femoral head asphericity plus acetabular overcoverage. Femoral head translation was seen close to the limit of motion during flexion-abduction-external rotation and anterior impingement exams. In particular the cam FAI patient had dramatic posteroinferior translation [59], which was evidence for the "levering" effect. Translation at this point has been theorized to increase loading on the posteroinferior acetabular

cartilage (opposite the contact or levering location) and has been termed the "contre-coup" effect. It was, however, not clear if any "contre-coup" joint contact occurred in the cam hip.

### Pelvic Kinematics

In an ex vivo study of 12 cadaver hips, applied internal rotation torque beyond 12 N.m produced motion of the pubic symphysis in native hips that suggested contact between the femur and acetabulum (Fig. 4.11) [61]. The addition of simulated

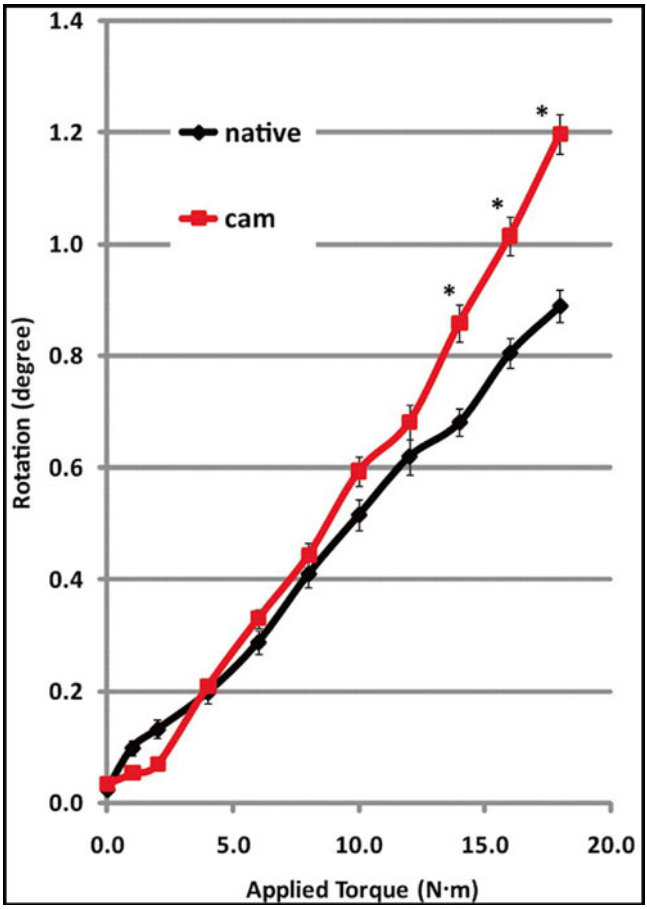


**Fig. 4.11** Mean transverse plane rotation of the pubic symphysis as a function of applied internal rotation torque for native and simulated cam deformity in cadaver hips. [Reprinted from Birmingham PM, Kelly BT, Jacobs R, McGrady L, Wang M. The Effect of Dynamic Femoroacetabular Impingement on Pubic Symphysis Motion: A Cadaveric Study. Am J Sports Med [Internet]. 2012 May [cited 2014 Jun 17];40(5):1113–8. With permission from Sage Publications.]

cam deformities to each native hip changed the pattern of pubic symphysis motion, suggesting altered contact between femur and acetabulum.

In an in vivo study, a group of 15 patients with cam FAI had decreased sagittal pelvic inclination in a squatting activity compared to 11 controls ($14.7 \pm 8.4°$ for cams versus $24.2 \pm 6.8°$ for controls). This finding was independent of squat depth. Since pelvic inclination brings the anterosuperior portion of the acetabulum close to the femoral neck, this may explain the decrease in pelvic inclination for the cam FAI group. It is not clear whether the observed decrease in pelvic inclination was compensatory or driven by bony impingement. Interestingly, there were no differences in hip joint angles at maximal squat depth [62].

### Joint Fluid Pressure

Joint fluid sealing ability was reduced in four cam-type hips with chondrolabral damage compared to six normal controls during pivoting activities but not in stooping or gait [63].

### Stress

A finite element model based on idealized geometry predicted that simulated cam deformity size ($\alpha$ angle) had no effect on peak contact stress or acetabular cartilage stress during walking [34]. However, at deep flexion during stand-to-sit, larger cam deformities led to higher joint contact stresses given normal acetabular geometry (at $\alpha = 40°$, peak contact stress was 3.66 MPa versus 8.84 MPa at $\alpha = 80°$). The highest peak joint contact stress, 16.51 MPa, was observed at the highest $\alpha$ angle in combination with a high CE angle (mixed-type impingement morphology). Acetabular cartilage stress was also greatest with the highest $\alpha$ angle and highest CE angle.

Subject-specific finite element models of two hips from patients with large cam deformities ($\alpha = 83°$ for both) and related symptoms, and two hips from matched normals ($\alpha = 42°$, $45°$) were combined with subject specific squat kinematics that had been gathered in a separate study [62] to evaluate locations and magnitudes of stress in acetabular cartilage and underlying subchondral bone in functional positions (standing and maximum squat) [38]. Cartilage stresses were higher in the cam patients than in the controls. The biggest difference between cam and control hips was found in underlying bone during squatting: in cam deformity hips, peak maximum bone shear stress was 13.4 and 16.9 MPa in the cam hips versus 4.4 and 4.5 MPa in the control hips.

A patient-specific finite element model was combined with subject specific ROM of one pathological pure-cam FAI hip ($\alpha = 98°$) and one control ($\alpha = 48°$) to predict contact stresses for three positional tests: 90° flexion, 24° internal rotation, and combined internal rotation at 90° flexion [64]. Cam deformity raised peak contact stress substantially relative to the control hip: peak contact stress was 6.60 MPa

(flexion) and 6.04 MPa (internal rotation) compared to 9.65 MPa (flexion) and 11.68 MPa (rotation) in the cam hip.

#### Subchondral Bone Density

In an in vivo quantitative computed tomography study, symptomatic and asymptomatic cam-deformity groups ($n = 12$ for all groups) had greater bone density in the anterosuperior acetabular region than controls by 14–35 % and 15–34 %, respectively [65]. Bone mineral density had a mild positive correlation with alpha angle. The increase in bone density may reflect repeated engagement between the deformed femur and the acetabulum.

## Biomechanical Effect of Poor Congruency

### *Perthes' Disease*

Legg-Calvé-Perthes disease (Perthes' or LCPD) is a childhood disorder where a loss of blood flow to the femoral head leads to necrosis and frequently results in residual deformity upon healing. The effect of joint deformity in the healed stage of Perthes' hips on joint contact stress is of particular concern because of the higher risk of early hip osteoarthritis in Perthes' patients.

#### Range of Motion

Perthes' hips had reduced abduction and all combinations of internal/external rotation with flexion or extension compared to normal hips (Fig. 4.12) [10]. The reduction of internal rotation was more marked than that of external rotation. Flexion, extension, and adduction were similar to results from normal children.

Joint preserving surgery increased ROM in all directions except flexion (average loss of 1° ROM) in 50 hips in 50 Perthes' patients at a mean of 8.2 years of follow-up, although changes were small (smallest: +2.3° mean adduction, largest: +7° mean external rotation) [66].

To help determine the cause of loss of ROM in Perthes', 27 patients, 6–10 years old (average 7.9 years) with early Perthes' disease who failed non-operative management and had normal ROM in the contralateral hip were examined for ROM both pre-operatively and under anesthesia [67]. Twenty-one of twenty-seven patients (77.7 %) had ROM of the Perthes' hip within 5° of the contralateral when examined under anesthesia and the remaining six patients had reduced abduction (<50°). The author speculated that pain and muscle spasm, rather than deformity and impingement, were the cause of loss of ROM in this population.

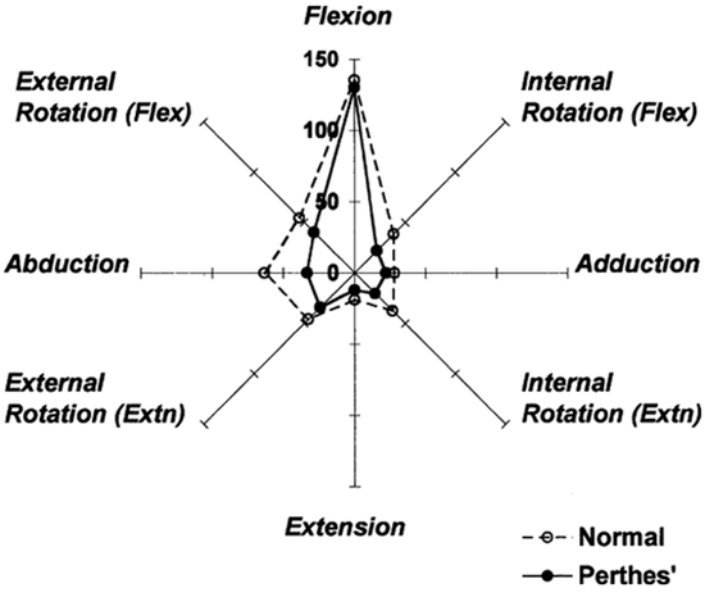


**Fig. 4.12** Range of motion in normal hips and hips with Perthes' disease. [Reprinted from Rao KN, Joseph B. Value of Measurement of Hip Movements in Childhood Hip Disorders. J Pediatr Orthop [Internet]. 2001;21(4):495–501. With permission from Wolters Kluwer Health.]

In a different approach to understanding loss of ROM in Perthes' disease, geometric models of 13 hips with Perthes' (41 years old, 22–69, Stulberg grades III–V) were compared to 27 normal hips (54 years old, 31–74). Hips with Perthes' disease had a reduced ROM in all movements (e.g., flexion: Perthes' 103 ± 40° (26–144), normal 125 ± 13° (103–146)). The location of impingement was also different, with a majority of Perthes' hips in an anterior impingement test simulation having femoral intra-articular (79 %) and extra-articular (86 %) impingement, compared to normal hips (15 % and 15 %, respectively). The primary limitation of this approach was that soft tissue, including cartilage and labrum, were not simulated, which would likely limit ROM prior to bony impingement in some cases.

## Stress

Models of 135 patients predicted that there was no difference in peak joint contact stress (normalized by body weight) between Perthes' and contralateral hips (2940 ± 885 versus 2946 ± 793 $m^{-2}$, respectively). There was a difference in the normalized values of contact stress gradient index (defined as the gradient magnitude at the lateral acetabular rim) between Perthes' and contralateral hips (4334 ± 51,011 versus −37,959 ± 35,848 $m^{-3}$, respectively), where the difference in sign is a result of the peak contact stress for a normal contralateral hip lying medial to the lateral

acetabular rim (resulting in a negative gradient as defined in this study—contact stress increases medially, and then decreases after the peak), and the peak contact stress for a Perthes' hip being at the lateral acetabular rim (resulting in a positive gradient as defined in this study—contact stress decreases medially). Models were based on simplified representations of the hip geometry based on 2D radiographs.

### Joint Fluid Pressure

Joint fluid pressure, measured in various joint positions (several with traction) under sedation using an arterial pressure transducer in 94 hips (81 children) was significantly lower in Perthes' hips than in other conditions (mean of three positions: Perthes' 2.8 kPa ($n=9$), transient synovitis 9.8 kPa ($n=74$), septic arthritis 10.1 kPa ($n=4$), reactive arthritis 16.0 kPa ($n=2$), arthritis with urticaria 20.3 kPa ($n=3$)) [68].

### Cartilage and Bone Material Properties

In a piglet model of Perthes' disease, Perthes' hips had lower bone stiffness (80 % lower) and yield strength (50 % lower) compared to the contralateral hip at 8 weeks, as well as a 31 % increase in bone collagen and a 25 % decrease in bone mineral content [69]. Perthes' hips also had lower cartilage stiffness (54 % lower) and yield strength (34 % lower) compared to contralateral hips at 8 weeks, although no differences were found in overall glycosaminoglycan concentration [69].

## *Coxa Magna*

Coxa magna, defined as overgrowth of the femoral head and neck, can be a sequela of Perthes' disease, transient synovitis, congenital hip dislocation, septic arthritis, osteomyelitis, juvenile rheumatoid arthritis, and trauma [70]. Coxa magna is frequently assessed by comparing the affected and contralateral sides using such criteria as an increase in femoral diameter of greater than 10 % [70] or a femoral head ratio of less than 0.9 (unaffected head diameter/affected head diameter) [71]. The thickening of the femoral neck means that this condition may also be categorized as resulting in poor clearance [72]. Although these findings strongly suggest that coxa magna modifies joint biomechanics, no studies that quantify this effect are available in the literature.

## Conclusions

It is surprising how little is known about hip biomechanics, given the prevalence of hip arthritis, the importance of biomechanics to many types of arthritis, and how much more is known about the biomechanics of other joints. The limited number

of experimental studies, both in vivo and ex vivo, is of particular concern. Model predictions must be treated with caution. While models make simulating diseases, deformities and surgical procedures possible, few biomechanical models have ever been shown to make reliable predictions of real measurements.

Overall it is clear that many hip conditions reduce joint range of motion. The evidence does not appear clear whether these reductions in range of motion are due to bony impingement or soft tissue changes. Models predict that hip disorders change contact pressure as would be predicted intuitively, and that surgical procedures like osteotomies have the desired effect on contact pressure. However there is very limited experimental evidence to back up these predictions or quantify them reliably.

## References

1. Wilson DR, McWalter EJ, Johnston JD. The measurement of joint mechanics and their role in osteoarthritis genesis and progression. Med Clin North Am [Internet]. 2009 [cited 2014 Sep 19];93(1):67–82, x. Available from: http://www.ncbi.nlm.nih.gov/pubmed/19059022
2. Smith MV, Panchal HB, Ruberte Thiele RA, Sekiya JK. Effect of acetabular labrum tears on hip stability and labral strain in a joint compression model. Am J Sports Med [Internet]. 2011 [cited 2014 Sep 27];39 Suppl:103S–10S. Available from: http://www.ncbi.nlm.nih.gov/pubmed/21709039
3. Myers CA, Register BC, Lertwanich P, Ejnisman L, Pennington WW, Giphart JE, et al. Role of the acetabular labrum and the iliofemoral ligament in hip stability: an in vitro biplane fluoroscopy study. Am J Sports Med [Internet]. 2011 [cited 2014 Sep 27];39 Suppl:85S–91S. Available from: http://www.ncbi.nlm.nih.gov/pubmed/21709037
4. Safran MR, Giordano G, Lindsey DP, Gold GE, Rosenberg J, Zaffagnini S, et al. Strains across the acetabular labrum during hip motion: a cadaveric model. Am J Sports Med [Internet]. 2011 [cited 2014 Oct 2];39 Suppl:92S–102S. Available from: http://www.ncbi.nlm.nih.gov/pubmed/21709038
5. Dy CJ, Thompson MT, Crawford MJ, Alexander JW, McCarthy JC, Noble PC. Tensile strain in the anterior part of the acetabular labrum during provocative maneuvering of the normal hip. J Bone Joint Surg Am [Internet]. 2008 [cited 2014 Jun 17];90(7):1464–72. Available from: http://www.ncbi.nlm.nih.gov/pubmed/18594094
6. Ferguson SJ, Bryant JT, Ganz R, Ito K. An in vitro investigation of the acetabular labral seal in hip joint mechanics. J Biomech [Internet]. 2003 [cited 2014 May 23];36(2):171–8. Available from: http://linkinghub.elsevier.com/retrieve/pii/S0021929002003652
7. Greaves LL, Gilbart MK, Yung AC, Kozlowski P, Wilson DR. Effect of acetabular labral tears, repair and resection on hip cartilage strain: a 7T MR study. J Biomech. 2010;43(5):858–63.
8. Weinstein SL, Mubarak SJ, Wenger DR. Fundamental concepts of developmental dysplasia of the hip. Instr Course Lect. 2014;63:299–305.
9. Peters CL, Erickson JA, Anderson L, Anderson AA, Weiss J. Hip-preserving surgery: understanding complex pathomorphology. J Bone Joint Surg Am [Internet]. 2009 [cited 2014 Jun 24];91 Suppl 6:42–58. Available from: http://www.pubmedcentral.nih.gov/articlerender.fcgi?artid=3347478&tool=pmcentrez&rendertype=abstract
10. Rao KN, Joseph B. Value of measurement of hip movements in childhood hip disorders. J Pediatr Orthop [Internet]. 2001;21(4):495–501. Available from: http://www.ncbi.nlm.nih.gov/pubmed/11433163
11. Pompe B, Antolič V, Mavčič B, Iglič A, Kralj-iglič V. Hip joint contact stress as an additional parameter for determining hip dysplasia in adults: comparison with Severin's classification. Med Sci Monit. 2007;13(5):215–9.

12. Zhao X, Chosa E, Totoribe K, Deng G. Effect of periacetabular osteotomy for acetabular dysplasia clarified by three-dimensional finite element analysis. J Orthop Sci [Internet]. 2010 [cited 2014 Jun 24];15(5):632–40. Available from: http://www.ncbi.nlm.nih.gov/pubmed/20953924
13. Genda E, Iwasaki N, Li G, MacWilliams BA, Barrance PJ, Chao EY. Normal hip joint contact pressure distribution in single-leg standing – effect of gender and anatomic parameters. J Biomech [Internet]. 2001;34(7):895–905. Available from: http://www.ncbi.nlm.nih.gov/pubmed/11410173
14. Hadley NA, Brown TD, Weinstein SL. The effects of contact pressure elevations and aseptic necrosis on the long-term outcome of congenital hip dislocation. J Orthop Res. 1990;8(4):504–13.
15. Maxian TA, Brown TD, Weinstein SL. Chronic stress tolerance levels for human articular cartilage: two nonuniform contact models applied to long-term follow-up of CDH. J Biomech. 1994;28(2):159–66.
16. Vukasinovic Z, Spasovski D, Kralj-Iglic V, Marinkovic-Eric J, Seslija I, Zivkovic Z, et al. Impact of triple pelvic osteotomy on contact stress pressure distribution in the hip joint. Int Orthop [Internet]. 2013 [cited 2014 Jun 24];37(1):95–8. Available from: http://www.pubmedcentral.nih.gov/articlerender.fcgi?artid=3532627&tool=pmcentrez&rendertype=abstract
17. Hsin J, Saluja R, Eilert RE, Wiedel JD. Evaluation of the biomechanics of the hip following a triple osteotomy of the innominate bone. J Bone Joint Surg Am [Internet]. 1996;78(6):855–62. Available from: http://www.ncbi.nlm.nih.gov/pubmed/8666603
18. Kralj M, Mavcic B, Antolic V, Iglic A, Kralj-Iglic V. The Bernese periacetabular osteotomy: clinical, radiographic and mechanical 7-15-year follow-up of 26 hips. Acta Orthop [Internet]. 2005 [cited 2014 Jun 24];76(6):833–40. Available from: http://www.ncbi.nlm.nih.gov/pubmed/16470438
19. Pfeifer R, Hurschler C, Ostermeier S, Windhagen H, Pressel T. In vitro investigation of biomechanical changes of the hip after Salter pelvic osteotomy. Clin Biomech (Bristol, Avon) [Internet]. 2008 [cited 2014 Jun 24];23(3):299–304. Available from: http://www.ncbi.nlm.nih.gov/pubmed/18023513
20. Tannast M, Siebenrock KA, Anderson SE. Femoroacetabular impingement: radiographic diagnosis – what the radiologist should know. Am J Roentgenol [Internet]. 2007 [cited 2013 Jan 31];188(6):1540–52. Available from: http://www.ncbi.nlm.nih.gov/pubmed/17515374
21. Tonnis D, Heinecke A. Acetabular and femoral anteversion: relationship with osteoarthritis of the hip. J Bone Joint Surg Am. 1999;81-A(12):1747–70.
22. Ganz R, Parvizi J, Beck M, Leunig M, Nötzli H, Siebenrock KA. Femoroacetabular impingement: a cause for osteoarthritis of the hip. Clin Orthop Relat Res [Internet]. 2003 [cited 2012 Oct 26];(417):112–20. Available from: http://www.ncbi.nlm.nih.gov/pubmed/14646708
23. Ganz R, Gill TJ, Gautier E, Ganz K, Krügel N, Berlemann U. Surgical dislocation of the adult hip. J Bone Joint Surg Am. 2001;83-B(8):1119–24.
24. Tannast M, Goricki D, Beck M, Murphy SB, Siebenrock KA. Hip damage occurs at the zone of femoroacetabular impingement. Clin Orthop Relat Res [Internet]. 2008 [cited 2013 Feb 5];466(2):273–80. Available from: http://www.pubmedcentral.nih.gov/articlerender.fcgi?artid=2505146&tool=pmcentrez&rendertype=abstract
25. Reynolds D, Lucas J, Klaue K. Retroversion of the acetabulum. J Bone Joint Surg Am. 1999;81-B:281–8.
26. Siebenrock KA, Schoeniger R, Ganz R. Anterior femoro-acetabular impingement due to acetabular retroversion: treatment with periacetabular osteotomy. J Bone Joint Surg Am. 2003;85-A(2):278–86.
27. Siebenrock KA, Kalbermatten DF, Ganz R. Effect of pelvic tilt on acetabular retroversion: a study of pelves. Clin Orthop Relat Res. 2003;407:241–8.
28. Dandachli W, Islam SU, Liu M, Richards R, Hall-Craggs M, Witt J. Three-dimensional CT analysis to determine acetabular retroversion and the implications for the management of femoro-acetabular impingement. J Bone Joint Surg Am [Internet]. 2009 [cited 2013 Feb 1];91(8):1031–6. Available from: http://www.ncbi.nlm.nih.gov/pubmed/19651829

29. Hansen BJ, Harris MD, Anderson LA, Peters CL, Weiss JA, Anderson AE. Correlation between radiographic measures of acetabular morphology with 3D femoral head coverage in patients with acetabular retroversion. Acta Orthop [Internet]. 2012 [cited 2014 Jun 17];83(3):233–9. Available from: http://www.pubmedcentral.nih.gov/articlerender.fcgi?artid=3369147&tool=pmcentrez&rendertype=abstract
30. Wyss TF, Clark JM, Weishaupt D, Nötzli HP. Correlation between internal rotation and bony anatomy in the hip. Clin Orthop Relat Res [Internet]. 2007 [cited 2013 Feb 5];460(460):152–8. Available from: http://www.ncbi.nlm.nih.gov/pubmed/17290151
31. Tannast M, Kubiak-Langer M, Langlotz F, Puls M, Murphy SB, Siebenrock KA. Noninvasive three-dimensional assessment of femoroacetabular impingement. J Orthop Res. 2007;25:122–31.
32. Kubiak-Langer M, Tannast M, Murphy SB, Siebenrock KA, Langlotz F. Range of motion in anterior femoroacetabular impingement. Clin Orthop Relat Res [Internet]. 2007 [cited 2014 Jul 29];458:117–24. Available from: http://www.ncbi.nlm.nih.gov/pubmed/17206102
33. Ross JR, Nepple JJ, Philippon MJ, Kelly BT, Larson CM, Bedi A. Effect of changes in pelvic tilt on range of motion to impingement and radiographic parameters of acetabular morphologic characteristics. Am J Sports Med [Internet]. 2014 [cited 2014 Aug 3]; Available from: http://www.ncbi.nlm.nih.gov/pubmed/25060073
34. Chegini S, Beck M, Ferguson SJ. The effects of impingement and dysplasia on stress distributions in the hip joint during sitting and walking: a finite element analysis. J Orthop Res [Internet]. 2009 [cited 2014 Jun 18];27(2):195–201. Available from: http://www.ncbi.nlm.nih.gov/pubmed/18752280
35. Harris MD, Anderson AE, Henak CR, Ellis BJ, Peters CL, Weiss JA. Finite element prediction of cartilage contact stresses in normal human hips. J Orthop Res [Internet]. 2012 [cited 2013 Feb 5];30(7):1133–9. Available from: http://www.ncbi.nlm.nih.gov/pubmed/22213112
36. Henak CR, Ateshian GA, Weiss JA. Finite element prediction of transchondral stress and strain in the human hip. J Biomech Eng [Internet]. 2014 [cited 2014 Jun 17];136(2):021021. Available from: http://www.ncbi.nlm.nih.gov/pubmed/24292495
37. Henak CR, Carruth ED, Anderson AE, Harris MD, Ellis BJ, Peters CL, et al. Finite element predictions of cartilage contact mechanics in hips with retroverted acetabula. Osteoarthritis Cartilage [Internet]. Elsevier Ltd; 2013 [cited 2014 Jun 17];21(10):1522–9. Available from: http://www.ncbi.nlm.nih.gov/pubmed/23792188
38. Ng KCG, Rouhi G, Lamontagne M, Beaulé PE. Finite element analysis examining the effects of cam FAI on hip joint mechanical loading using subject-specific geometries during standing and maximum squat. HSS J [Internet]. 2012 [cited 2014 Jun 17];8(3):206–12. Available from: http://www.pubmedcentral.nih.gov/articlerender.fcgi?artid=3470675&tool=pmcentrez&rendertype=abstract
39. Brown TD, Shaw DT. In vitro contact stress distributions in the natural human hip. J Biomech [Internet]. 1983;16(6):373–84. Available from: http://www.ncbi.nlm.nih.gov/pubmed/6619156
40. Tubby AH. Coxa valga (collum valgum). Proc R Soc Med. 1908;1:107–42.
41. Haverkamp D, Marti RK. Bilateral varus osteotomies in hip deformities: are early interventions superior? A long-term follow-up. Int Orthop [Internet]. 2007 [cited 2014 Jul 30];31(2):185–91. Available from: http://www.pubmedcentral.nih.gov/articlerender.fcgi?artid=2267573&tool=pmcentrez&rendertype=abstract
42. Siebenrock KA, Steppacher SD, Haefeli PC, Schwab JM, Tannast M. Valgus hip with high antetorsion causes pain through posterior extraarticular FAI. Clin Orthop Relat Res [Internet]. 2013 [cited 2014 Jun 18];471(12):3774–80. Available from: http://www.ncbi.nlm.nih.gov/pubmed/23463288
43. Günther CMJ, Komm M, Jansson V, Heimkes B. Midterm results after subtrochanteric end-to-side valgization osteotomy in severe infantile coxa vara. J Pediatr Orthop [Internet]. 2013;33(4):353–60. Available from: http://www.ncbi.nlm.nih.gov/pubmed/23653021
44. Fairbank HAT. Coxa vara due to congenital defect of the neck of the femur. Anatomy. 1928;62(Pt 2):232–7.

45. Rhyu KH, Kim YH, Park WM, Kim K, Cho T-J, Choi IH. Application of finite element analysis in pre-operative planning for deformity correction of abnormal hip joints – a case series. Proc Inst Mech Eng H [Internet]. 2011 [cited 2014 Jun 24];225(9):929–36. Available from: http://pih.sagepub.com/lookup/doi/10.1177/0954411911407247
46. Mamisch TC, Kim Y-J, Richolt JA, Millis MB, Kordelle J. Femoral morphology due to impingement influences the range of motion in slipped capital femoral epiphysis. Clin Orthop Relat Res [Internet]. 2009 [cited 2014 Jun 24];467(3):692–8. Available from: http://www.pubmedcentral.nih.gov/articlerender.fcgi?artid=2635459&tool=pmcentrez&rendertype=abstract
47. Murray RO. The aetiology of primary osteoarthritis of the hip. Br J Radiol. 1965;38(455):810–24.
48. Solomon L. Patterns of osteoarthritis of the hip. J Bone Joint Surg Am. 1976;58-B(2):176–83.
49. Ganz R, Leunig M, Leunig-Ganz K, Harris WH. The etiology of osteoarthritis of the hip: an integrated mechanical concept. Clin Orthop Relat Res [Internet]. 2008 [cited 2014 Jul 10];466(2):264–72. Available from: http://www.pubmedcentral.nih.gov/articlerender.fcgi?artid=2505145&tool=pmcentrez&rendertype=abstract
50. Ito K, Minka M, Leunig M, Werlen S, Ganz R. Femoroacetabular impingement and the cam-effect. J Bone Joint Surg Br. 2001;83(B):171–6.
51. Nötzli HP, Wyss TF, Stoecklin CH, Schmid MR, Treiber K, Hodler J. The contour of the femoral head-neck junction as a predictor for the risk of anterior impingement. J Bone Joint Surg Br [Internet]. 2002;84(4):556–60. Available from: http://www.ncbi.nlm.nih.gov/pubmed/12043778
52. Jäger M, Wild A, Westhoff B, Krauspe R. Femoroacetabular impingement caused by a femoral osseous head-neck bump deformity: clinical, radiological, and experimental results. J Orthop Sci [Internet]. 2004 [cited 2014 Jul 27];9(3):256–63. Available from: http://www.ncbi.nlm.nih.gov/pubmed/15168180
53. Strehl A, Ganz R. Anterior femoroacetabular impingement after healed femoral neck fractures. Unfallchirurg [Internet]. 2005 [cited 2014 Aug 16];108(4):263–73. Available from: http://www.ncbi.nlm.nih.gov/pubmed/15785946
54. Krekel PR, Vochteloo AJ, Bloem RM, Nelissen RG. Femoroacetabular impingement and its implications on range of motion: a case report. J Med Case Rep [Internet]. BioMed Central Ltd; 2011 [cited 2013 Feb 5];5(1):143. Available from: http://www.pubmedcentral.nih.gov/articlerender.fcgi?artid=3079675&tool=pmcentrez&rendertype=abstract
55. Kapron AL, Anderson AE, Peters CL, Phillips LG, Stoddard GJ, Petron DJ, et al. Hip internal rotation is correlated to radiographic findings of cam femoroacetabular impingement in collegiate football players. Arthroscopy [Internet]. Elsevier Inc.; 2012 [cited 2013 Feb 5];28(11):1661–70. Available from: http://www.ncbi.nlm.nih.gov/pubmed/22999076
56. Audenaert E, Van Houcke J, Maes B, Vanden Bossche L, Victor J, Pattyn C. Range of motion in femoroacetabular impingement. Acta Orthop Belg [Internet]. 2012;78(3):327–32. Available from: http://www.ncbi.nlm.nih.gov/pubmed/22822572
57. Audenaert EA, Peeters I, Vigneron L, Baelde N, Pattyn C. Hip morphological characteristics and range of internal rotation in femoroacetabular impingement. Am J Sports Med [Internet]. 2012 [cited 2013 Feb 5];40(6):1329–36. Available from: http://www.ncbi.nlm.nih.gov/pubmed/22472271
58. Audenaert EA, Mahieu P, Pattyn C. Three-dimensional assessment of cam engagement in femoroacetabular impingement. Arthroscopy [Internet]. Elsevier Inc.; 2011 [cited 2014 Jun 17];27(2):167–71. Available from: http://www.ncbi.nlm.nih.gov/pubmed/20952150
59. Kapron AL, Aoki SK, Peters CL, Anderson AE. In vivo hip kinematics during clinical exams using dual fluoroscopy and model-based tracking: application to the study of femoroacetabular impingement. Orthopaedic Research Society Annual Meeting. New Orleans, LA; 2014. p. 242.
60. Kapron AL, Aoki SK, Peters CL, Maas SA, Bey MJ, Zauel R, et al. Accuracy and feasibility of dual fluoroscopy and model-based tracking to quantify in vivo hip kinematics during clinical exams. J Appl Biomech. 2014;30:461–70.

61. Birmingham PM, Kelly BT, Jacobs R, McGrady L, Wang M. The effect of dynamic femoroacetabular impingement on pubic symphysis motion: a cadaveric study. Am J Sports Med [Internet]. 2012 [cited 2014 Jun 17];40(5):1113–8. Available from: http://www.ncbi.nlm.nih.gov/pubmed/22392561
62. Lamontagne M, Kennedy MJ, Beaulé PE. The effect of cam FAI on hip and pelvic motion during maximum squat. Clin Orthop Relat Res [Internet]. 2009 [cited 2013 Feb 4];467(3):645–50. Available from: http://www.pubmedcentral.nih.gov/articlerender.fcgi?artid=2635464&tool=pmcentrez&rendertype=abstract
63. Dwyer MK, Jones HL, Field RE, McCarthy JC, Noble PC. Femoroacetabular impingement negates the acetabular labral seal during pivoting maneuvers but not gait. Clin Orthop Relat Res [Internet]. 2014 [cited 2014 Jul 25]; Available from: http://www.ncbi.nlm.nih.gov/pubmed/24989124
64. Jorge JP, Simões FMF, Pires EB, et al. Finite element simulations of a hip joint with femoro-acetabular impingement. Comput Methods Biomech Biomed Engin. 2014;17(11):1275–84.
65. Speirs AD, Beaulé PE, Rakhra KS, Schweitzer ME, Frei H. Increased acetabular subchondral bone density is associated with cam-type femoroacetabular impingement. Osteoarthr Cartil [Internet]. Elsevier Ltd; 2013 [cited 2014 Jun 17];21(4):551–8. Available from: http://www.ncbi.nlm.nih.gov/pubmed/23357224
66. Albers CE, Steppacher SD, Ganz R, Siebenrock KA, Tannast M. Joint-preserving surgery improves pain, range of motion, and abductor strength after Legg-Calvé-Perthes disease. Clin Orthop Relat Res [Internet]. 2012 [cited 2014 Jun 16];470(9):2450–61. Available from: http://www.pubmedcentral.nih.gov/articlerender.fcgi?artid=3830093&tool=pmcentrez&rendertype=abstract
67. Stanitski CL. Hip range of motion in Perthes' disease: comparison of pre-operative and intra-operative values. J Child Orthop [Internet]. 2007 [cited 2013 Jul 29];1(1):33–5. Available from: http://www.pubmedcentral.nih.gov/articlerender.fcgi?artid=2656703&tool=pmcentrez&rendertype=abstract
68. Kallio P, Ryoppy S. Hyperpressure in juvenile hip disease. Acta Orthop Scand. 1985; 56(3):211–4.
69. Koob TJ, Pringle D, Gedbaw E, Meredith J, Berrios R, Kim HKW. Biomechanical properties of bone and cartilage in growing femoral head following ischemic osteonecrosis. J Orthop Res. 2007;25(6):750–7.
70. Young EY, Gebhart JJ, Bajwa N, Cooperman DR, Ahn NU. Femoral head asymmetry and coxa magna: anatomic study. J Pediatr Orthop [Internet]. 2014;34(4):415–20. Available from: http://www.ncbi.nlm.nih.gov/pubmed/24322627
71. Larson AN, Sucato DJ, Herring JA, Adolfsen SE, Kelly DM, Martus JE, et al. A prospective multicenter study of Legg-Calve-Perthes disease. J Bone Joint Surg Am. 2012;94(7):584–92.
72. Anderson LA, Erickson JA, Severson EP, Peters CL. Sequelae of Perthes disease: treatment with surgical hip dislocation and relative femoral neck lengthening. J Pediatr Orthop [Internet]. 2010;30(8):758–66. Available from: http://www.pubmedcentral.nih.gov/articlerender.fcgi?artid=3031125&tool=pmcentrez&rendertype=abstract.